Cement and Concrete Research 48 (2013) 116–127

Contents lists available at SciVerse ScienceDirect

Cement and Concrete Research

journal homepage: http://ees.elsevier.com/CEMCON/default.asp

The apparent and effective chloride migration coefficients obtained in migration tests

P. Spiesz *, H.J.H. Brouwers

Department of the Built Environment, Eindhoven University of Technology, P. O. Box 513, 5600 MB Eindhoven, The Netherlands

ARTICLE INFO

Article history:
Received 22 August 2012
Accepted 15 February 2013
Available online xxxx

Keywords:
Diffusion (C)
Chloride (D)
Transport properties (C)
Modeling (E)
Durability (C)

ABSTRACT

The apparent (D_{app}) and effective (D_{eff}) migration coefficients obtained in chloride migration tests are investigated in this study. The presented D_{app} profiles in concrete show that the apparent migration coefficient is strongly concentration-dependent. As demonstrated, the binding of chlorides during the migration tests is very low at low free-chloride concentrations and therefore the chloride penetration front progresses throughout the concrete only slightly retarded by the binding. The diffusion flux during migration tests is shown to be insignificant compared to the migration flux. The D_{RCM} obtained from the Rapid Chloride Migration (RCM) tests are found to be equal to the computed D_{app} at the locations of the chloride penetration fronts, which gives an indication that the D_{RCM} represents only the migration coefficient at the front. A linear correlation is found between the D_{RCM} obtained from the traditional RCM model and the D_{eff} obtained from the chloride transport model which includes non-linear chloride binding and concentrations in non-equilibrium.

1. Introduction

Chloride induced corrosion of steel rebars is the main cause of deterioration of concrete elements and structures being exposed to chloride bearing environments. Therefore, it is of vital importance to design new structures with minimized risk of this type of deterioration. The concrete cover, which is the layer of concrete that separates the steel rebars from the external environment, plays a crucial role in resisting the ingress of chlorides during a certain time (so-called service lifetime), after which the critical chloride concentration is reached at the level of the rebars so that the corrosion of the steel is triggered. Two main properties of the concrete cover determine the service lifetime of concrete: its thickness and permeability to chlorides, and both these properties may be adjusted in order to meet the service lifetime criteria in the design stage. Chloride ingress speed in concrete is diffusion controlled and in order to quantify it various test methods can be used. In the past, mainly the natural diffusion test methods were used, but nowadays the importance and applicability of accelerated migration tests have significantly increased. Chloride migration tests were developed to obtain the chloride diffusion coefficient in a much shorter test period compared to natural diffusion tests, by accelerating the chloride ingress rate with the applied electrical field. The chloride transport process in concrete during electrically forced migration in transient conditions can be described by the Nernst–Planck equation, as follows [1,2]:

$$\frac{\partial c}{\partial t} = D_0\left(\frac{\partial^2 c}{\partial x^2} - \frac{zFE}{RT}\frac{\partial c}{\partial x}\right) \quad (1)$$

where: c — free-chloride concentration, t — time, D_0 — intrinsic chloride migration coefficient, x — distance, z — ionic valence, F — Faraday constant, E — electric field, R — universal gas constant and T — temperature. The Nernst–Planck equation shown in the present form Eq. (1) can be termed simplified, as it assumes a linear decay of the applied potential in the sample, a constant value of the chloride diffusion/migration coefficient, a negligible effect of ionic activities and no advection. Because the coefficient D_0 in Eq. (1) is obtained from chloride migration tests, it is often called "migration coefficient" to differentiate it from the diffusion coefficient obtained in diffusion tests [3]. Tang [3,4] explains that these two coefficients are not the same because of different counter-electrical potentials (caused by differences in drift velocities of cations and anions in pore solution) and ionic frictions during diffusion and migration processes.

The intrinsic migration coefficient D_0 in Eq. (1) represents the diffusion/migration rate of chlorides in the pore solution of concrete, i.e. it does not refer to the overall volume of concrete but just to its liquid phase, and therefore is related to the diffusivity of chlorides in free liquid constrained by the pore structure of the porous medium (its tortuosity and constrictivity). In order to quantify the chloride diffusion/migration coefficient referring not only to the volume of pores, but to

* Corresponding author. Tel.: +31 40 247 5904; fax: +31 40 243 8595.
E-mail address: p.spiesz@tue.nl (P. Spiesz).

0008-8846/$ – see front matter © 2013 Elsevier Ltd. All rights reserved.
http://dx.doi.org/10.1016/j.cemconres.2013.02.005

the total volume of concrete, the effective and apparent diffusion/migration coefficients are used. The effective chloride diffusion/migration coefficient refers to the diffusivity of chlorides in the pore solution by taking into account the volume fraction of the permeable pores in the entire volume of concrete (i.e. porosity) [5]:

$$D_{eff} = \varphi \cdot \frac{\delta}{\tau^2} D_f = \varphi D_0 \tag{2}$$

where: D_{eff} — effective chloride diffusion/migration coefficient, φ — total water-permeable porosity, δ — constrictivity of pore structure, τ — tortuosity of pore structure, D_f — chloride diffusion coefficient in free liquid (infinite dilution) and D_0 — intrinsic chloride diffusion/migration coefficient in pore solution. The effective diffusion/migration coefficients are determined in steady-state diffusion/migration tests, i.e. with a constant chloride flux (c is independent of distance and time). Nevertheless, steady-state tests are often not preferred from the practical point of view as they are time consuming and laborious (the upstream chloride solution must be periodically replaced and the concentration of chlorides in the downstream solution must be regularly measured). To overcome these drawbacks, non-steady-state chloride diffusion and migration tests were developed. The apparent diffusion/migration coefficients obtained in the non-steady-state tests represent the diffusion/migration of chlorides in the pore solution of concrete, taking into account the reaction between the chlorides and the porous medium (so-called chloride binding). Following Atkinson and Nickerson [5], assuming that the effective diffusion coefficient is independent of the free-chloride concentration, the apparent chloride diffusion/migration coefficient can be defined as follows:

$$D_{app} = \frac{\varphi}{\lambda} \cdot \frac{\delta}{\tau^2} D_f = \frac{\varphi}{\lambda} D_0 = \frac{D_{eff}}{\lambda} \tag{3}$$

where: D_{app} — apparent chloride diffusion/migration coefficient and λ — distribution coefficient of chlorides between the solid and liquid. The distribution coefficient can be further defined as [5,6]:

$$\lambda = \varphi\left(1 + \frac{\partial c_b}{\partial c}\right) \tag{4}$$

where: c_b — bound-chloride concentration [g_{Cl}/dm^3_{liquid}] and c — free-chloride concentration [g_{Cl}/dm^3_{liquid}].

Combining Eqs. (3) and (4), the following relationship can be derived [1,5,6]:

$$D_{app} = \frac{D_0}{1 + \frac{\partial c_b}{\partial c}} = \frac{D_{eff}}{\varphi\left(1 + \frac{\partial c_b}{\partial c}\right)} \tag{5}$$

The apparent chloride diffusion/migration coefficient, as shown in Eq. (5), depends on the chloride binding capacity defined as $\partial c_b/\partial c$, i.e. the ability of concrete to bind further chlorides when the free-chloride concentration increases [1,6]. As can be seen in Eq. (5), the D_{app} can be equal to the D_0 or D_{eff}/φ in two cases: *i*) if there is no chloride binding (as e.g. for inert porous media) and *ii*) if chloride binding is completed (as e.g. during steady-state chloride diffusion/migration tests).

Tang [3] shows that the relationship between the D_{app} and D_{eff}, given in Eq. (5), should also include the concentration dependency of the chloride migration coefficient, as follows:

$$D_{app} = \frac{D_{eff} + \left(\frac{RT}{zFE}\frac{\partial c}{\partial x} + c\right)\frac{\partial D_{eff}}{\partial c}}{\varphi\left(1 + \frac{\partial c_b}{\partial c}\right)}. \tag{6}$$

It is known that the effective chloride migration coefficient is a function of the concentration [3,4,7–9]; nevertheless, for the sake of simplicity, in chloride transport models the migration coefficients are assumed to be independent of the free-chloride concentration. In such a case Eq. (6) can be simplified to Eq. (5), as for example adopted in Tang's chloride migration transport model for the Rapid Chloride Migration (RCM) test [1,10].

The non-steady-state chloride migration coefficient, which is obtained in the RCM test, is based on the simplified Nernst–Planck equation (Eq. (1)) and reads [1]:

$$\frac{\partial c}{\partial t} = D_{RCM}\left(\frac{\partial^2 c}{\partial x^2} - \frac{zFE}{RT}\frac{\partial c}{\partial x}\right) \tag{7}$$

and

$$D_{RCM} = D_{app} = \frac{D_0}{1 + \frac{\partial c_b}{\partial c}} = \frac{D_{eff}}{\varphi\left(1 + \frac{\partial c_b}{\partial c}\right)} = constant. \tag{8}$$

The assumption of a constant binding capacity $\partial c_b/\partial c$ in Eq. (8) is very questionable as it only represents the case when chloride binding follows a linear isotherm (i.e. $c_b = A \cdot c$, where A is a binding constant) and is in instantaneous equilibrium. The binding of chlorides is a very complex process because different hydrated cement phases are able to bind different amounts of chloride, in different ways (chemically or physically) and at different rates [11]. In fact, chloride binding obeys the non-linear Freundlich isotherm (i.e. $c_b = K_b \cdot c^n$, where K_b and n are binding constants) very well in a wide concentration range of c, as demonstrated in [1]. Fig. 1a shows the chloride binding curve determined experimentally by Zibara [12] (units of concentrations were recalculated to the units used in this paper) for an OPC paste with w/c ratio of 0.3, fit to both Freundlich and linear isotherms. These measurements represent the equilibrium between the free- and bound-chloride concentrations, reached within about two weeks. Fig. 1b shows the $\partial c_b/\partial c$ term derived for the isotherms given in Fig. 1a. It can be seen that for the linear binding isotherm the binding capacity is constant, which obeys the assumption adopted in Eq. (8). In the case of the Freundlich isotherm, the binding capacity is concentration dependent and is much larger for lower c than for larger c. In the case of short-term chloride migration tests, the duration of which most often amounts to just 24 h [10], the term $\partial c_b/\partial c$ in Eqs. (5) and (8) becomes even more complicated as the concentrations are obviously in non-equilibrium. In the literature, the equilibrium concentration for chloride binding is reported to be reached between seven days up to two months of exposure [1,12,13]. These facts give evidence that the chloride migration coefficient D_{RCM}, as defined in Eq. (8), will not be constant, but instead, will depend on the local free- and bound-chloride concentrations in the concrete sample.

In this article, the apparent chloride migration coefficient obtained in the Rapid Chloride Migration test is estimated along the depth of the tested concrete sample, to investigate if/how its value changes during the test. Both our own test results and empirical data obtained from the literature are used. The chloride transport model presented in Spiesz et al. [14] is firstly extended by adding a non-zero chloride flux due to the diffusion (in the original model that flux was neglected) and then applied to experimental data, to compute the effective chloride migration coefficient as well as the free-, bound- and total-chloride concentration profiles after the migration tests. From the effective chloride diffusion coefficient and the term $\partial c_b/\partial c$ (see Eq. (5)), the D_{app} is computed. Additionally, this computed D_{app} is verified against the D_{RCM} obtained from the traditional RCM test model.

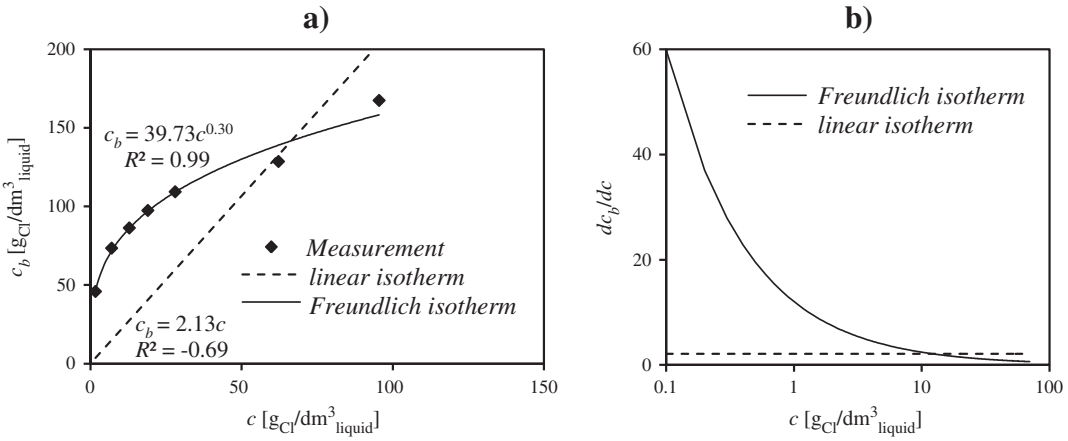

Fig. 1. a) Chloride binding data fit to Freundlich and linear isotherms; b) chloride binding capacity (dc_b/dc) computed for Freundlich and linear isotherms.

2. Employed chloride transport model

The employed chloride transport model for the RCM tests, developed in Spiesz et al. [14], takes into account the non-linear nature of chloride binding and non-equilibrium conditions between the free- and bound-chloride concentrations. Due to the questionably constant value of the apparent chloride migration coefficient (D_{RCM}) in the traditional RCM model (see previous paragraph), the effective coefficient is adopted instead in the new model. The D_{eff} is independent of chloride binding and is related only to the diffusion/migration of chloride in free liquid and to the porosity of concrete (see Eq. (2)). The model is based on the simplified Nernst–Planck equation (Eq. (1)) and is split into two equations describing individually the chloride concentrations in liquid and solid states. It is assumed that the binding of chlorides takes place instantaneously at the surface of the hardened cement paste (i.e. reaction kinetics do not limit the chloride transport), but there is resistance to the mass transfer through the stagnant liquid at the liquid–solid interface. This limitation in the mass transfer rate of chlorides is responsible for the non-equilibrium conditions in the system and is governed by the mass transfer coefficient — k. The mass transfer rate of chlorides is proportional to the deviation of the chloride concentration in the pore solution from the equilibrium concentration at the liquid–solid interface, as given by the Freundlich equation [14].

The following assumptions are adopted in the employed chloride transport model [14]: (i) no convection; (ii) diffusion and migration of chlorides only in the pore solution of concrete; (iii) one dimensional and constant electrical field distribution in the concrete sample; (iv) non-linear chloride binding; (v) non-equilibrium between free- and bound-chloride concentrations; (vi) constant binding parameters and (vii) negligible effect of ionic interactions during the test. The diffusion flux is often neglected in chloride transport models for migration tests because it is much smaller compared to the migration flux [1,14]. Nevertheless, in the present work, the chloride transport model given in [14] has been extended by adding a non-zero chloride diffusion flux to improve its accuracy. The model reads for the liquid and solid phases respectively:

$$\varphi\frac{\partial c}{\partial t} - D_{eff}\left(\frac{\partial^2 c}{\partial x^2} - \frac{zFE}{RT}\frac{\partial c}{\partial x}\right) = -k\left[c - \left(\frac{C_b}{K_b}\right)^{1/n}\right] \tag{9}$$

$$(1-\varphi)\rho_s\frac{\partial C_b}{\partial t} = k\left[c - \left(\frac{C_b}{K_b}\right)^{1/n}\right] \tag{10}$$

with the following initial and boundary conditions:

$$\begin{aligned} &C_b(x, t=0) = C_{bi} \\ &c(x=0, t) = c_0 \\ &c(x=\infty, t) = 0 \end{aligned} \tag{11}$$

where: C_b — bound chloride concentration [g_{Cl}/g_{solid}], K_b and n — binding parameters from the Freundlich isotherm, ρ_s — specific density of concrete, C_{bi} — initial bound-chloride concentration [g_{Cl}/g_{solid}] and c_0 — chloride concentration in the bulk liquid [g_{Cl}/dm^3_{liquid}].

From the practical point of view it is very difficult to measure the free- or bound-chloride concentration profiles in concrete; therefore, the total chloride concentration (C_t) is usually measured. The relationship between the concentrations c and C_b in Eqs. (9) and (10) and C_t reads as follows [14]:

$$C_t = \frac{c\varphi + C_b(1-\varphi)\rho_s}{\rho_a}\cdot 100 \tag{12}$$

where: C_t — total chloride concentration in concrete [$g_{Cl}/100g_{concrete}$] and ρ_a — apparent density of concrete.

As demonstrated by Tang in [3,4], the chloride diffusion coefficient is not equal to the migration coefficient because the counter-electrical potentials (caused by differences in drift velocities of cations and anions in pore solution) and ionic frictions during diffusion and migration processes are not the same. Therefore, one can consider the Nernst–Planck equation (Eq. (1)), including two different coefficients: i) the diffusion coefficient, related to the transport of chlorides due to the concentration gradient and ii) migration coefficient, related to the transport of chloride due to the application of electrical field, and in such a case Eq. (9) can be rewritten as follows:

$$\varphi\frac{\partial c}{\partial t} - D^*_{eff}\frac{\partial^2 c}{\partial x^2} + D_{eff}\frac{zFE}{RT}\frac{\partial c}{\partial x} = -k\left[c - \left(\frac{C_b}{K_b}\right)^{1/n}\right] \tag{13}$$

where: D^*_{eff} — effective chloride diffusion coefficient and D_{eff} — effective chloride migration coefficient.

3. Application to experimental data

Experimental results used in this study include our own experimental data [16] as well as data retrieved from the literature [15,17]. The mix proportions and properties of analyzed concretes (5 different mixes) and mortar are presented in Table 1. Concrete/mortar disks of 50 mm in height and 100 mm in diameter were tested following the RCM test procedure described in the NT Build 492 [10] guideline. The tests were performed at different experimental

Table 1
Mix proportions and properties of the analyzed concretes.

Mix number	C1 [15]	C2 [15]	C3 [16]	C4 [17]	C5 [17]	C6 [17]
	Composition [kg/m^3]					
Cement	418	363	786	400	380	363
Water	146	163	207	140	182	218
Coarse aggregates	1025	1025	–	1281	1217	1162
Sand	695	698	1382	660	627	599
w/c	0.35	0.45	0.26	0.35	0.48	0.60
age [months]	12–18	12–18	1	2	2	2
σ_c[a][MPa]	52	33	97.8	81.7	46.7	37.9
ρ_a [kg/m^3]	2577	2553	2450	2637	2608	2584
ρ_s [kg/m^3]	2601	2606	2710	2665	2661	2643
φ [-]	0.113	0.143	0.150	0.102	0.141	0.150
Cement type	T10	T10	CEM I 52.5 N	CEM I 52.5 N	CEM I 52.5 N	CEM I 52.5 N

[a] 28 days for C3; 56 days otherwise.

conditions, as specified in Table 2. The total water permeable porosity of concrete was measured using the vacuum-saturation technique and the total-chloride concentration profiles after the RCM test were measured in ground layers of concrete sample using the potentiometric titration method. The details of both measurement procedures are described in [15–17].

The system of Eqs. (9)–(11) is a system of partial non-linear differential equations with the non-linearity coming from the reaction term. This system consists of a second order partial differential equation coupled with an ordinary differential equation. Due to the non-linearities, for the coupled system, an explicit solution is difficult to obtain. Thus, the problem was solved numerically in Matlab. For time-discretization the following were chosen: $N \in N$, the time step $\zeta = t_{RCM}/N$ and $t_i = i \cdot \zeta$, $i = \{1,\ldots,N\}$, so that the time discretization was uniform. The solution pair $(c_i, C_{b,i})$ is a numerical approximation of the solution pair (c, C_b) at time t_i. Starting with the initial conditions $(c_I, C_{b,I})$ and for given $(c_{i-1}, C_{b,i-1})$, the semi-implicit time discretization leads to the following equations for the free- and bound-chlorides respectively:

$$\varphi\frac{c_i - c_{i-1}}{\zeta} - D_{eff}\frac{\partial^2 c_i}{\partial x^2} + \frac{D_{eff} zFE}{RT}\frac{\partial c_i}{\partial x} = -k\left[c_i - \left(\frac{C_{b,i-1}}{K_b}\right)^{1/n}\right] \tag{14}$$

$$(1-\varphi)\rho_s C_{b,i} = (1-\varphi)\rho_s C_{b,i-1} + \zeta k\left[c_i - \left(\frac{C_{b,i-1}}{K_b}\right)^{1/n}\right]. \tag{15}$$

The above problems are de-coupled when c_i is solved using Eq. (14), and then, due to an explicit discretization in Eq. (15), $C_{b,i}$ can be computed directly. For the transport equation (Eq. (14)) a finite difference method on 3-point stencil was employed to discretize in space. For the time discretization, as can be seen from Eq. (14), the Euler explicit method for the reaction term and the implicit method for the convective and diffusive terms were used. For the ordinary differential equation, as shown in Eq. (15), the free-chloride concentration c_i computed above was used and Euler explicit time stepping was used to compute the bound-chloride concentration. The total chloride concentration was computed by the expression given in Eq. (12).

The data given in Tables 1 and 2 (φ, ρ_a, ρ_s, U, c_0, t_{RCM}) were used along with the total chloride concentration profiles (measured in the samples after the test) in the optimization process of the unknown model parameters (D_{eff}, k, K_b and n, see Eqs. (9) and (10)). The following interval constraints were used in the optimization of the parameters (based on [14]): $D_{eff} \in (0.1 \cdot 10^{-12}, 3.0 \cdot 10^{-12})$ m^2/s, $k \in (0.5 \cdot 10^{-6}, 3.0 \cdot 10^{-5})$ 1/s, $n \in (0.4, 0.6)$ and $K_b \in (1 \cdot 10^{-4}, 1 \cdot 10^{-3})$ dm^{3n}/g^n. The initial bound-chloride concentration C_{bi} (see Eq. (11)) was set equal to the background concentration measured for each analyzed chloride profile. Differently from the previous work of the authors [14], the system of Eqs. (9)–(12) was solved applying a more precise value of the bulk chloride concentration c_0 (1.83 mol/dm^3 instead of 2 mol/dm^3 used e.g. in [1,14]).

In the optimization process, the total mean square error of the difference between the measured and simulated total chloride concentration profiles was minimized by adjusting the values of k, K_b, n and D_{eff}. The error was calculated applying the following formula:

$$error = \sqrt{\frac{\sum_{i=1}^{j}\left(C_{t\_\mathrm{mod}} - C_{t\_mea}\right)^2}{j}} \tag{16}$$

where: j — number of measured data points, C_{t_mod} — total chloride concentration obtained from the model at a defined depth and C_{t_mea} — total chloride concentration measured at a defined depth.

3.1. Diffusion flux of chloride during migration test

The system of equations describing the chloride transport during the migration test (Eqs. (9) and (10)) was solved with the term $D_{eff} \cdot \partial^2 c/\partial x^2$ set equal and unequal to zero, to investigate the influence of the diffusion flux on the total chloride transport process during the migration test. Additionally, the equation for the transport of chlorides employing separate chloride diffusion and migration coefficients (Eq. (13)) was solved to investigate if these two coefficients had the same values. Fig. 2 shows the optimized total chloride concentration profiles for concrete C1 at different experimental conditions (C1a–c, see Table 2). The values of the optimized parameters corresponding to the profiles shown in Fig. 2 are given in Table 3. Optimization of the parameters for concretes C2–C6 (see Table 1) was also performed and the results are shown in Table 4.

One can notice from Fig. 2 and Table 3 that the optimized chloride concentration profiles and the corresponding parameters are almost identical for all the investigated cases: neglected diffusion flux and non-zero diffusion flux with the migration coefficient equal/unequal to the diffusion coefficient. This tendency gives evidence that during the RCM test, the diffusion flux of chlorides due to the concentration gradient is insignificant compared to the electrically-induced flux. This confirms the assumption adopted in the chloride transport model used in this study and also in many other models (e.g. [1,18–21]). In the case of independent optimization of the chloride migration and diffusion coefficients (D_{eff} and D_{eff}^* respectively), one can notice in Table 3 that the optimized values of D_{eff}^* are in the same order of magnitude as the D_{eff}, but slightly lower. Nevertheless, because the influence of the chloride diffusion flux on the total flux is minimal (as shown in Fig. 2), the value of D_{eff}^* does not alter the optimized chloride concentration profile or the optimization error, so the accuracy of the optimization of D_{eff}^* is also low.

Table 2
RCM test conditions.

	C1 a	C1 b	C1 c	C2 a	C2 b	C2 c	C3 a	C3 b	C3 c	C4	C5	C6
t_{RCM} [h]	6	9	18	6	9	18	24	24	24	24	24	24
U [V]	60	60	60	60	60	60	35	47.5	60	35	25	20
c_0 [g$_{Cl}$/dm^3$_{liquid}$]	64.95	64.95	64.95	64.95	64.95	64.95	64.95	64.95	64.95	64.95	64.95	64.95

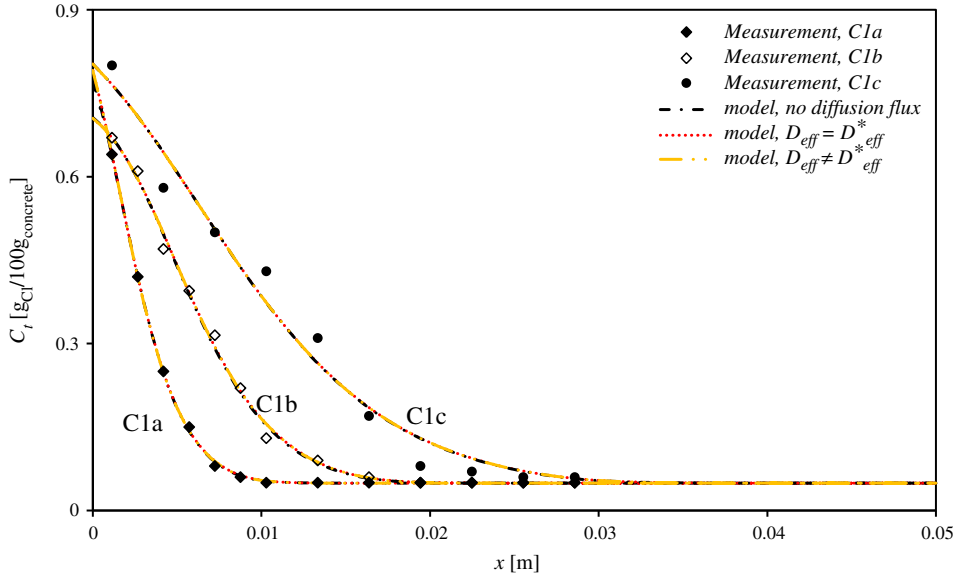

Fig. 2. Measured and computed total chloride concentration profiles for concrete C1a–c, with and without considering the chloride diffusion flux during migration.

Table 3
Optimized parameters for concrete C1a–c for three cases: no diffusion flux and with the diffusion flux when $D_{eff} = D^*_{eff}$ and $D_{eff} \neq D^*_{eff}$. The corresponding computed chloride profiles are shown in Fig. 2.

	No diffusion flux, $D^*_{eff} = 0$				
	D_{eff} [$\cdot 10^{12}$ m^2/s]	k [$\cdot 10^6$ 1/s]	K_b [$\cdot 10^4$ dm^{3n}/g^n]	n –	Error (Eq. (16))
C1a	0.81	14.36	6.70	0.53	0.004
C1b	1.05	9.95	5.83	0.51	0.015
C1c	0.97	5.16	5.50	0.57	0.039
	With diffusion flux, $D_{eff} = D^*_{eff}$				
	D_{eff} [$\cdot 10^{12}$ m^2/s]	k [$\cdot 10^6$ 1/s]	K_b [$\cdot 10^4$ dm^{3n}/g^n]	n –	Error (Eq. (16))
C1a	0.81	14.36	6.70	0.54	0.005
C1b	1.05	9.92	6.05	0.50	0.015
C1c	0.97	5.16	5.50	0.57	0.039
	With diffusion flux, $D_{eff} \neq D^*_{eff}$				
	D_{eff} [$\cdot 10^{12}$ m^2/s]	D^*_{eff} [$\cdot 10^{12}$ m^2/s]	k [$\cdot 10^6$ 1/s]	K_b [$\cdot 10^4$ dm^{3n}/g^n]	n –	Error (Eq. (16))
C1a	0.81	0.57	14.36	6.70	0.54	0.005
C1b	1.05	0.45	9.92	6.05	0.50	0.015
C1c	0.97	0.31	5.16	5.50	0.57	0.039

Table 4
Optimized parameters for concretes C1–C6.

	D_{eff} [$\cdot 10^{12}$ m^2/s]	k [$\cdot 10^6$ 1/s]	K_b [$\cdot 10^4$ dm^{3n}/g^n]	n –	Error (Eq. (16))
C1a	0.81	14.36	6.70	0.54	0.004
C1b	1.05	9.92	6.05	0.50	0.015
C1c	0.97	5.16	5.50	0.57	0.039
C2a	1.94	6.92	6.50	0.53	0.021
C2b	1.91	6.11	9.05	0.55	0.041
C2c	1.80	2.09	8.00	0.55	0.033
C3a	0.75	6.50	5.25	0.50	0.062
C3b	0.67	7.00	5.10	0.51	0.064
C3c	0.79	7.00	4.80	0.53	0.058
C4	0.65	3.10	5.00	0.49	0.035
C5	1.21	1.40	5.55	0.46	0.015
C6	2.22	0.74	8.05	0.53	0.033

3.2. Chloride binding capacity and the apparent chloride migration coefficient

In order to determine the apparent chloride migration coefficient, Eq. (5) was used. The D_{eff} and the free- and bound-chloride concentration profiles (c and C_b, respectively) were obtained by applying the model (Eqs. (9) and (10)) to the experimental data, as described previously. Since the unit of the C_b obtained in this optimization is g_{Cl}/g_{solid} and in the term $\partial c_b/\partial c$, needed for the calculation of the D_{app}, both concentrations should have consistent units (i.e. g_{Cl}/dm^3_{liquid}), the following equation was used to unify the units:

$$c_b = \frac{C_b \cdot \rho_a}{\varphi}. \quad (17)$$

As an example, Fig. 3a–c shows the optimized free-, bound- and total-chloride concentration profiles together with the measured total concentration profiles for concrete C1a–c. The parameters obtained from the data fitting for concrete C1a–c are given in Table 3 (for $D_{eff} = D_{eff}^{*}$). One can notice in Fig. 3a–c that the chloride profiles symmetrically progress further into the depth of concrete with time (6 h RCM test for C1a, 9 h for C1b and 18 h for C1c). Despite the different durations of the RCM tests performed on concrete C1a–c, the optimized parameters are relatively constant (see Table 3 for $D_{eff} = D_{eff}^{*}$). The only parameter whose optimized value varies significantly is the mass transfer coefficient k. This has been previously observed in [14]. It seems that the value of k diminishes in time, which means that the mass transfer of

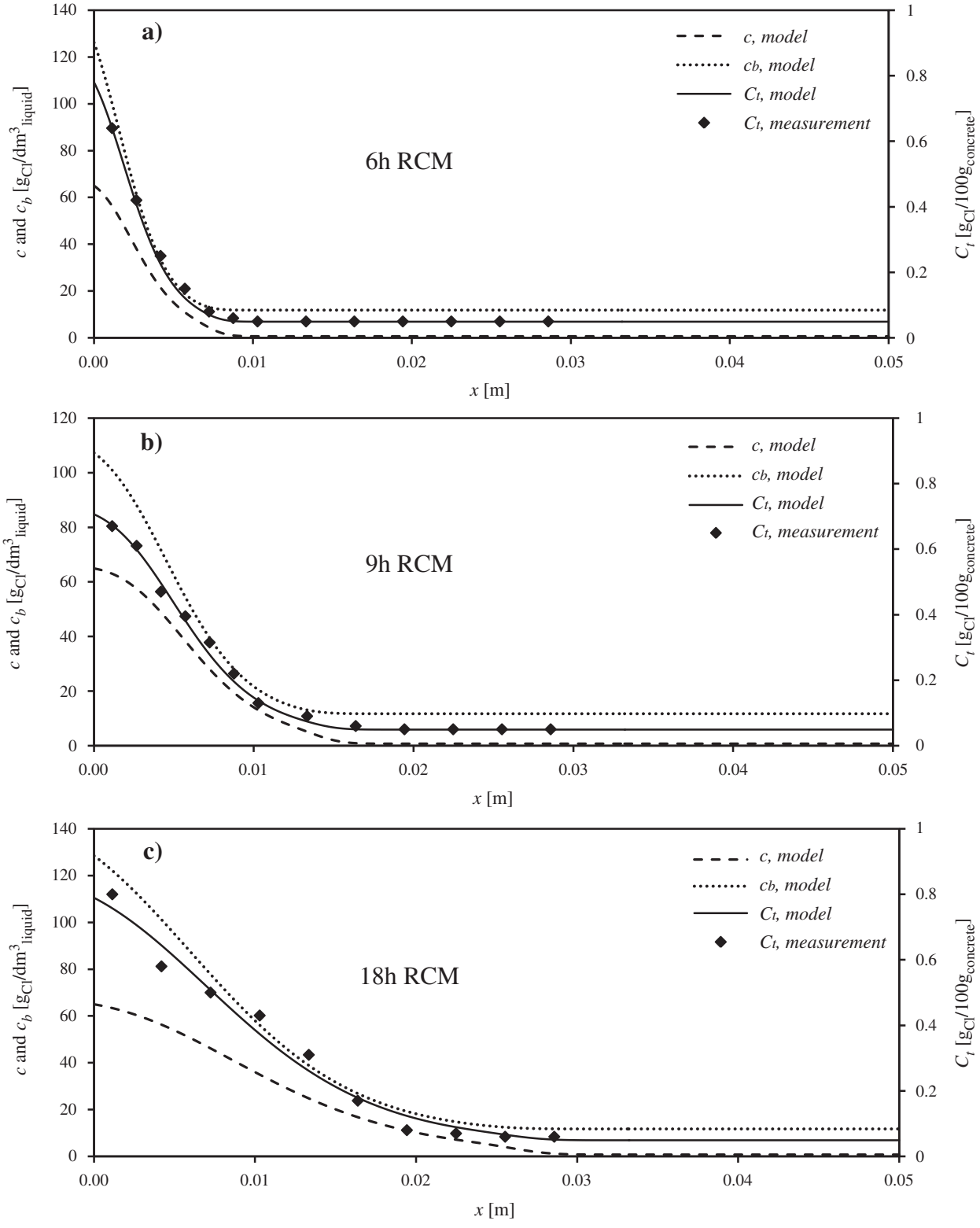

Fig. 3. Free-, bound- and total-chloride concentration profiles obtained from the model for concrete: a) C1a, b) C1b and c) C1c.

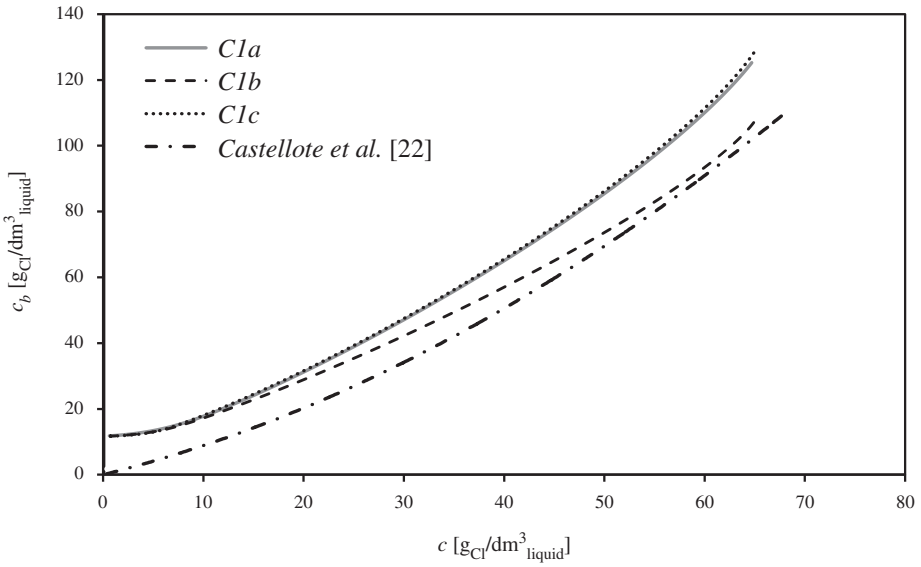

Fig. 4. Chloride binding isotherms computed from the model vs. the isotherm measured in [22].

chlorides from the liquid to the solid phase reduces when the duration of the test increases. This phenomenon still needs a closer investigation.

With known c_b and c profiles in concrete, the binding isotherm during the RCM test can be derived. Therefore, in Fig. 4 the chloride binding isotherms obtained from the model for concrete C1a–c are shown. As expected, these isotherms are very different from the Freundlich isotherm (see Fig. 1a), which was obtained in concentration–equilibrium conditions (i.e. when a sufficient time is given to complete binding). However, given a sufficient time, the isotherms shown in Fig. 4 should reach the Freundlich isotherm. It can be noticed, comparing the Freundlich isotherm (Fig. 1a) to the modeled isotherms (Fig. 4), that the binding of chlorides during migration tests is much lower for low free-chloride concentrations. This phenomenon has been also confirmed in [22,23]. The reduced binding at low c can be explained through the reaction model given in Eqs. (9) and (10). It can be noticed that in this model the reaction (binding) rate is proportional to the deviation of the chloride concentration in the bulk solution from the equilibrium concentration at the liquid–solid interface. Therefore, the deviation of c_b from the equilibrium concentration will be low for low values of c and it will increase proportionally with the increase of c. In turn, the increase in the amount of bound chlorides will be low at low c and respectively higher for larger c.

In Castellote et al. [22] an isotherm measured during non-steady-state migration test is reported, and is also shown in Fig. 4 (c_b was recalculated to the unit used in this work assuming $\rho_a = 2400$ g/dm^3 and $\varphi = 0.14$) for a comparison with the isotherms obtained from the model. It can be noticed that the predicted isotherms for concrete C1a–c and the one measured in [22] are similar, except for the region of low free-chloride concentrations. This difference can be explained by the fact that in the isotherms computed from the model the initial bound-chloride concentration is non-zero, but instead, it corresponds to the measured total chloride background concentration, while for the isotherm measured in [22] the initial c_b is zero. Besides the region of low c, both isotherms presented in Fig. 4 are in a very good agreement, which confirms the employed non-equilibrium binding model. Castellote et al. [22] explain that the isotherm determined after the migration test differs from a Freundlich isotherm because of the non-equilibrium conditions during the short-term migration tests. Additionally, the lower bound-chloride concentration is attributed to the faster transport rate of chlorides during migration compared to the diffusion transport rate, which in turn might cause binding to occur less.

The term $\partial c_b/\partial c$, needed for the estimation of D_{app} or D_{RCM} (Eqs. (5) and (8), respectively), was derived from the computed free- and bound-chloride concentration profiles, and is shown in Fig. 5a for concrete C1a–c. The binding capacity profiles in concrete C1a–c are given in Fig. 5b. Again, one can see in these figures that the binding capacity, defined as $\partial c_b/\partial c$, is much greater at higher free-chloride concentrations than at lower concentrations.

With the known porosities (from measurements), free- and bound-chloride concentration profiles and effective migration coefficients obtained from the model, it is possible to estimate the apparent migration coefficient profiles in concrete, applying Eq. (5). Fig. 6a–b show the computed D_{app} profiles obtained for concrete C1 and C2, respectively, for which the test conditions were the same, except for the duration (i.e. 6 h, 9 h and 18 h of the RCM test at 60 V). Fig. 6c shows the D_{app} profiles obtained for mortar C3a–c, for which the duration of the test was the same for all the tested samples (24 h), but the applied voltages were different (35 V, 47.5 V and 60 V). Fig. 6d shows the D_{app} profiles obtained for three concretes with different w/c ratios (0.35, 0.48 and 0.6). The D_{app} profiles given in Fig. 6a–d are computed until the depth of the free-chloride penetration (the so-called chloride penetration front). All the derived D_{app} profiles have a similar characteristic: lower values of the D_{app} in the layers of concrete closer to the exposed surface (higher chloride concentrations), followed by a region of a rapid increase and finally a flat region with relatively constant D_{app} in the layers close to the chloride penetration front (very low chloride concentrations). As can be observed in Figs. 2 and 3, the chloride concentrations in concrete samples after the RCM test decrease gradually from high values at the exposed surfaces to zero in deeper layers. Due to these increased concentrations in the surface layers, the term $\partial c_b/\partial c$ is also larger in these layers (see Fig. 5a–b), which in turn reduces the value of the D_{app}, following Eq. (5). The regions of a rapid increase of the D_{app} in Fig. 6a–d correspond to the value of the binding capacity $\partial c_b/\partial c$, which changes significantly at low free-chloride concentrations (about 1–10 g_{Cl}/dm^3_{liquid}), as can also be seen in Fig. 5a–b. Therefore, in concrete layers with free-chloride concentrations in this range, the binding capacity varies greatly, which, according to Eq. (5) also greatly influences the D_{app}. For very low chloride concentrations the binding capacity is also low and it does not significantly influence the value of the D_{app}, which explains the flat region of the profiles in the vicinity of the chloride penetration front (see Fig. 6a–d). One can notice in Fig. 6a–d that in each

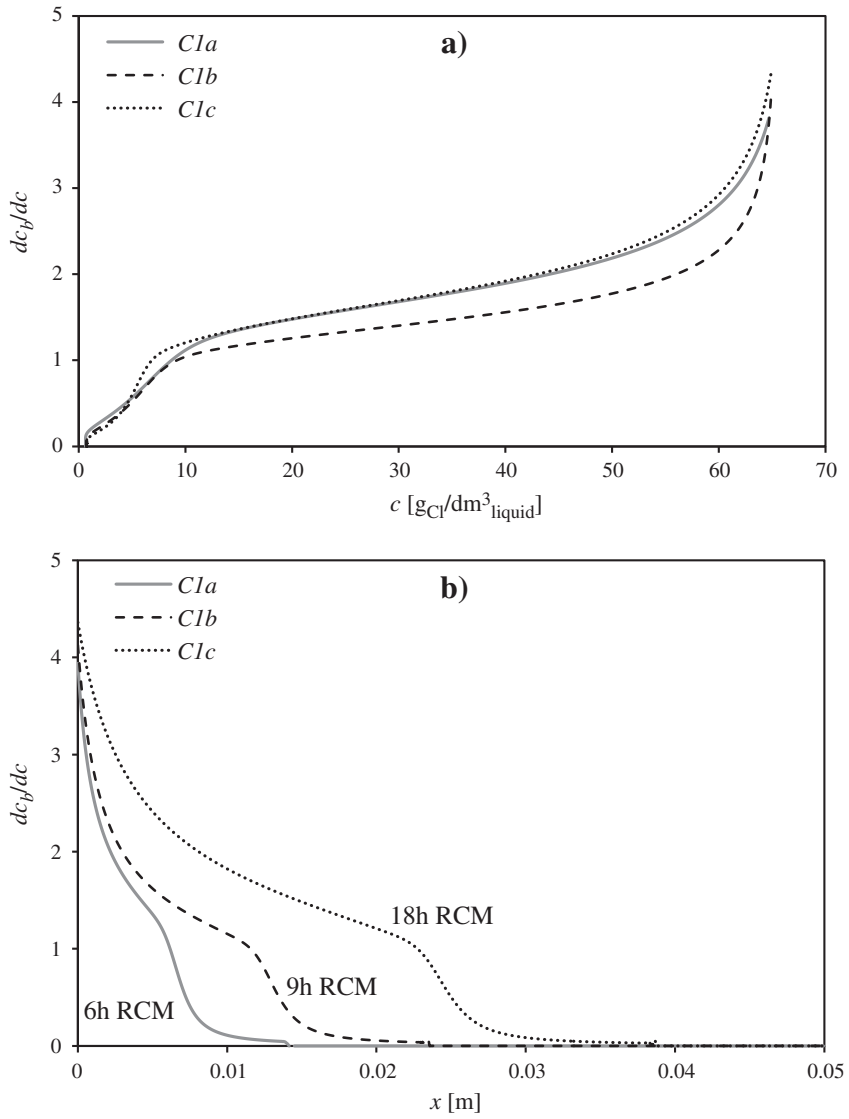

Fig. 5. a) Chloride binding capacity vs. free-chloride concentration and b) chloride binding capacity profile in concrete during the migration test.

profile the D_{app} is not constant as assumed in the traditional RCM test model [1], but instead varies greatly: the difference between the minimum values in the regions of concrete with high c and the maximum values in the vicinity of the chloride penetration front (at very low c), is of about a factor of four.

4. The migration coefficients D_{eff} and D_{RCM}

As demonstrated in the previous section, the apparent chloride migration coefficient during the short-term chloride migration test is not constant, but instead, due to non-linear binding and non-equilibrium conditions, it varies greatly within the concrete sample. This contradicts the assumption of a constant D_{RCM} (Eq. (8)), adopted in the RCM test chloride transport model.

Following the RCM test guideline [1,10], the chloride migration coefficient is calculated as follows:

$$D_{RCM} = \frac{RT}{zFE} \cdot \frac{x_d - \alpha\sqrt{x_d}}{t_{RCM}} \tag{18}$$

and

$$\alpha = 2\sqrt{\frac{RT}{zFE}} \cdot erf^{-1}\left(1 - \frac{2c_d}{c_0}\right) \tag{19}$$

where: α — laboratory constant, x_d — chloride penetration depth indicated by a colourimetric indicator, t_{RCM} — duration of the RCM test, erf — error function and c_d — chloride concentration at which the colourimetric indicator changes the color.

The values of the D_{RCM} computed from Eqs. (18) and (19) are shown in Table 5, together with the free-chloride penetration depths (x_d), which were used for their calculation. The values of x_d were derived from the computed free-chloride profiles, assuming that the colourimetric indicator for chlorides (0.1 mol/dm^3 $AgNO_3$ solution sprayed onto the split concrete samples after performing the RCM test) indicates a free-chloride concentration equal to 0.07 mol/dm^3 (2.48 g/dm^3) for an OPC concrete [1,24]. This concentration at the color-change boundary was also confirmed in [16] for an OPC mortar, however, many researchers reported larger values, especially in the case of concrete with slag cements [17,32,33].

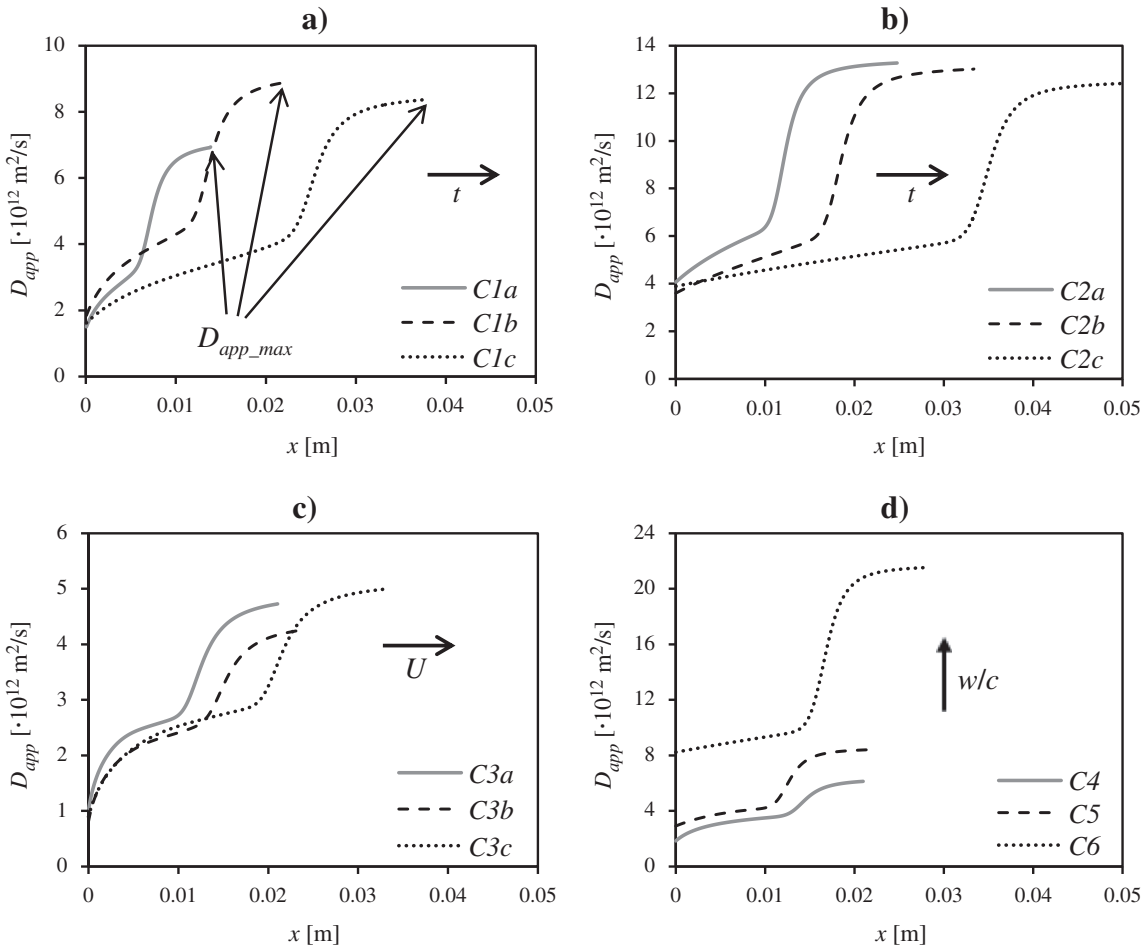

Fig. 6. The apparent chloride migration profiles during the chloride migration tests; a) C1a–c, b) C2a–c, c) C3a–c, and d) C4, C5 and C6.

The maximum values of the apparent chloride migration coefficient (D_{app_max}), obtained from the model for each derived profile shown in Fig. 6a–d, are also given in Table 5. These values represent the migration coefficient at very low free-chloride concentrations, right behind the progressing chloride penetration front in concrete, where the binding capacity is very low. It can be seen in the presented profiles that the D_{app_max} for the same concrete remains relatively constant at different durations of the test (Fig. 6a–b) and at different applied voltages (Fig. 6c). Following Eq. (5) it can be stated with a good approximation that the D_{app_max} equals the D_{eff}/φ or D_0, as the derived $\partial c_b/\partial c$ term is nearly zero for the migrating chloride penetration front (obtained minimum values of $\partial c_b/\partial c$ are in the range of 0.02–0.09 for the analyzed profiles). As shown in Table 5, the values of the D_{RCM} obtained from the traditional RCM model are very similar to the values of the D_{app_max} retrieved from the D_{app} profiles. This means that the D_{RCM} represents the apparent chloride migration coefficient in concrete only in the vicinity of the chloride penetration front (low values of c), where the binding of chlorides is very limited. As can be concluded from the binding isotherms shown in Figs. 4 and 5, the chloride penetration front can progress in concrete only slightly retarded by chloride binding. This influence becomes more significant when the chloride concentration increases, in which case, the value of the D_{app} behind the chloride penetration front decreases towards the exposed surface, where the D_{app} is the lowest (see Fig. 6a–d).

Table 5
Chloride migration coefficients from the RCM test (D_{RCM}) and the maximum apparent chloride apparent chloride migration coefficients (D_{app_max}) computed for concretes C1–C6.

	x_d [mm]	D_{RCM} [·10^{12} m^2/s]	D_{app_max} [·10^{12} m^2/s]
C1a	7.85	6.85	6.94
C1b	14.70	8.91	8.92
C1c	26.85	8.24	8.38
C2a	15.99	14.60	13.28
C2b	22.61	13.99	13.03
C2c	42.19	13.35	12.40
C3a	11.05	4.16	4.73
C3b	13.52	3.84	4.25
C3c	19.10	4.40	5.01
C4	15.70	6.08	6.12
C5	16.88	9.16	8.40
C6	23.54	16.45	21.53

In Spiesz et al. [14] it has been stated that the D_{RCM} calculated from the traditional RCM model (Eqs. (8), (18) and (19)) is larger than the D_{RCM} (or D_{app}) calculated from the D_{eff}, which was obtained either by fitting profiles (for non-steady-state regime experiments) or measured in steady-state regime migration tests. However, the equation used in [14] to correlate the D_{eff} and D_{RCM} employs only the maximum value of the binding capacity ($\partial c_b/\partial c$), which in turn gives only the minimum value of the D_{app} that can be observed in Fig. 6a–d in the surface layers of concrete. In the present article it is shown more properly that the D_{app} is not constant, but it changes within the concrete sample.

Based on the explanations given above, Eq. (8), which represents the D_{RCM} in the traditional RCM model [1], can be modified by

neglecting the chloride binding capacity for the migrating chloride penetration front:

$$D_{RCM} = D_{app\_max} \approx D_0 \approx \frac{D_{eff}}{\varphi} = constant. \quad (20)$$

The constant D_{app} assumed in the traditional RCM model (Eq. (8)) is correct, but not because of the constant binding capacity term assumed in this model, but due to the lack of chloride binding at very low chloride concentrations. One can notice that the D_{RCM} represents only one case of the D_{app}, i.e. when there is no chloride binding, and then it equals the D_{eff}/φ or D_0 (see Eqs. (5) and (20)). Therefore, the constant D_{RCM}, as defined in Eq. (8), is not valid in the entire volume of the tested concrete sample, but only in the vicinity of the chloride penetration front, where the binding is negligible. However, as the traditional D_{RCM} is determined based only on the position of the chloride penetration front, it should not be affected by the binding.

The correlation between the D_{RCM} and D_{eff} given in Eq. (20) is very straightforward — only the porosity is the proportional factor between the two coefficients. This relationship is presented in Fig. 7 for the data analyzed in this study. The linear correlation between the D_{RCM} and D_{eff} shown in Fig. 7 is clear, and the proportionality factor of 0.133 obtained in the regression can also be accurately predicted from the term $\varphi \cdot (1 + \partial c_b/\partial c)$ in Eq. (5), applying the weighted average porosities of all the analyzed concrete samples and the binding capacity term of 0.08.

Because the chloride penetration front during migration tests progresses at much higher rates compared to diffusion tests, Eq. (20) is not valid for long-term diffusion tests. As shown in Yuan [17] or Loser et al. [25], for the same concrete, the D_{RCM} is about 30% larger than the D_{app} obtained in the non-steady-state diffusion test [26]. This can be explained by the $\partial c_b/\partial c$ term, which will increase for the slowly diffusing chloride penetration front, and following Eq. (5) will decrease the D_{app_max}.

5. Discussion

The RCM test has received some criticism in the literature for the adapted chloride transport model. This criticism focused mainly on the difference between the theoretical and measured chloride concentration profiles after the test [14–17,27,28]. It was already mentioned in Tang [1], that the theoretical 'tsunami'-shape free-chloride concentration profile, in which the free-chloride concentration decreases from the maximum concentration (c_0) to zero within a very short distance in the concrete sample, is different from actually measured profiles. In these, the chloride concentration decreases gradually and is in fact very similar in shape to diffusion profiles measured after the natural diffusion tests. The gradual concentration profiles after the non-steady-state chloride migration tests were later experimentally confirmed by many researchers [14–17,27–33], and only in [34] the measured chloride concentration profile was similar to the theoretical one. Tang [1] lists the following hypotheses explaining the difference between the theoretical and experimental chloride profiles: i) different pore distribution resulting in different penetration fronts, thus the measured profile is a combination of these different penetrations; ii) the influence of other ions on the chloride binding or iii) reaction kinetics which change the shape of the profile without changing the penetration depth. For the latter argument an equation including a first-order chemical reaction model is used to represent the chloride binding rate through a linear binding isotherm [1,35]. Nevertheless, the simulated chloride profiles again do not match well with the measured ones [1]. Therefore, a new chloride transport model was proposed in Spiesz et al. [14], which considers the non-linear binding in non-equilibrium conditions and can predict the experimental profile much better than the traditional model. Based on the present article the explanation of the measured gradual profile can be extended: due to the mass transfer resistance of chlorides (concentration non-equilibrium) and non-linear chloride binding, the local binding capacity and therefore the local apparent chloride migration coefficient D_{app}, depend upon the local free- and bound-chloride concentrations. For the chloride penetration front, the binding capacity is very low so the front progresses through the concrete not retarded by the binding. On the other hand, the concentration behind the front increases, which in turn increases the binding capacity. Therefore, in the locations in concrete behind the chloride penetration front there is a larger deviation of bound-chloride concentration from the equilibrium concentration, so the binding takes place faster and reduces the D_{app}. Thus, at higher free-chloride concentrations more chlorides are bound, which causes a higher accumulation of the total-chlorides in the layers of concrete closer to the exposed concrete surface than in the deeper layers, closer to the chloride penetration front. However, this process does not significantly influence the chloride penetration front because at very low free-chloride concentrations the binding capacity is minimal. Therefore, the D_{RCM} determined in the migration tests based only on the position of the chloride front is not influenced by the chloride binding and as shown in the present study, equals the intrinsic chloride migration coefficient (D_0) and the effective chloride migration coefficient obtained from the model divided by the porosity of concrete.

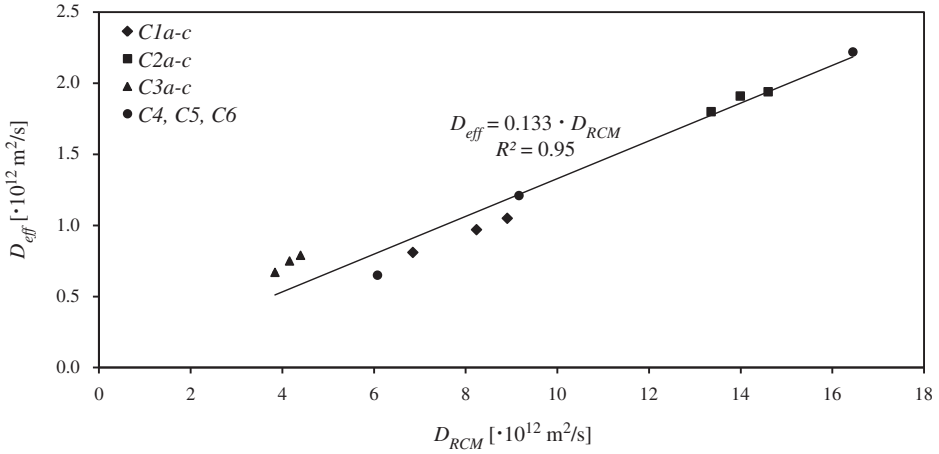

Fig. 7. The effective chloride migration coefficient obtained from the new model vs. the chloride migration coefficient obtained from the traditional RCM model.

6. Conclusions

The following conclusions can be drawn from the present article:

- This study increases the understanding of the chloride transport process during migration tests.
- The diffusion flux of chloride during the migration test can be neglected as the chloride transport is dominated by the electrically forced migration.
- The chloride binding capacity, defined as $\partial c_b/\partial c$, is not constant in the whole volume of concrete as assumed in the traditional RCM model. Due to the non-linear binding and non-equilibrium conditions between c and c_b, the binding capacity changes locally with the chloride concentrations.
- The binding capacity during migration tests is very low at low free-chloride concentrations. Hence, the progress of the free-chloride penetration front through the concrete sample during migration tests is not retarded by chloride binding. Therefore, the traditional D_{RCM}, computed based on the position of the chloride penetration front is not affected.
- The apparent chloride migration coefficient changes during the RCM test within the concrete sample, because it is a function of the local binding capacity. The computed D_{app} profiles show that the apparent migration coefficients are much higher at the chloride penetration front location (for very low c) and decrease towards the exposed surface (higher c).
- The chloride migration coefficient in the traditional RCM model is defined as a constant apparent migration coefficient. In fact, it represents only the maximum apparent migration coefficient which prevails at low c (in vicinity of the chloride penetration front). Therefore, the constant D_{RCM} is valid only at the location of the chloride penetration front and not in the regions of concrete in which the chloride concentrations are increased.
- The maximum values of the D_{app} computed from the proposed chloride transport model are very similar to the D_{RCM} computed from the traditional RCM model. Additionally, it is explained that the D_{RCM} is identical with the intrinsic chloride migration coefficient in the pore solution (D_0) and with the effective chloride migration coefficient (D_{eff}) divided by the porosity (D_{eff}/φ). A clear linear correlation between the obtained D_{RCM} and D_{eff} is found.
- The discrepancy between the theoretical abrupt chloride concentration profile and the experimental gradual profiles can be attributed to the fact that at higher chloride concentrations the chloride binding capacity is increased. This in turn reduces the apparent chloride migration coefficient in the layers of concrete with increased chloride concentrations, and causes a higher accumulation of chlorides in these layers compared to the layers with lower c (closer to the chloride penetration front).

List of symbols

c	concentration of chlorides in pore solution [g_{Cl}/dm^3_{liquid}]
c_b	concentration of bound-chloride [g_{Cl}/dm^3_{liquid}]
c_d	concentration of chlorides at which 0.1 N $AgNO_3$ changes color [g_{Cl}/dm^3_{liquid}]
c_0	concentration of chlorides in bulk solution [g_{Cl}/dm^3_{liquid}]
C_b	concentration of bound-chloride [g_{Cl}/g_{solid}]
C_{bi}	initial concentration of bound-chloride [g_{Cl}/g_{solid}]
C_t	total concentration of chlorides [$g_{Cl}/100g_{concrete}$]
C_{t_mea}	measured total concentration of chlorides [$g_{Cl}/100g_{concrete}$]
C_{t_mod}	total concentration of chlorides computed from the model [$g_{Cl}/100g_{concrete}$]
D_{app}	apparent chloride diffusion/migration coefficient [m^2/s]
D_{app_max}	maximum apparent chloride migration coefficient [m^2/s]
D_{eff}	effective chloride diffusion/migration coefficient [m^2/s]
D^*_{eff}	effective chloride diffusion coefficient [m^2/s]
D_f	chloride diffusion coefficient in free liquid [m^2/s]
D_{RCM}	chloride migration coefficient obtained from the traditional RCM test [m^2/s]
D_0	intrinsic chloride diffusion/migration coefficient in concrete pore solution [m^2/s]
E	electrical field [V/m]
F	Faraday constant, 96485 [C/mol]
i	number -
j	number of measured data points -
k	chloride mass transfer coefficient [1/s]
K_b	Freundlich isotherm binding constant [dm^{3n}/g^n]
L	thickness of concrete specimen [m]
n	Freundlich isotherm binding constant -
N	number -
R	universal gas constant, 8.314 [$Jmol^{-1}\ K^{-1}$]
t	time [s]
t_{RCM}	duration of the RCM test [s]
T	temperature [K]
U	electrical voltage [V]
w/c	water/cement ratio -
x	distance [m]
x_d	chloride penetration depth indicated by $AgNO_3$ [m]
z	ion valence -
α	laboratory constant for the RCM test -
δ	constrictivity of pore structure -
σ_c	compressive strength [MPa]
φ	total water-permeable porosity of concrete [%] or -
λ	distribution coefficient of chlorides between the solid and liquid -
ρ_a	apparent density of concrete [g/dm^3]
ρ_s	specific density of concrete [g/dm^3]
τ	tortuosity of pore structure -
ζ	time step in time-discretization [s]

Acknowledgments

The authors wish to express their gratitude to Dr. K. Kumar (TU Eindhoven/University of Texas) for his help with numerical solutions of the partial differential equations, to Dipl. Ing. M.V.A. Florea (TU Eindhoven) for her editorial help, to ir. J.J.W. Gulikers (Rijkswaterstaat Centre for Infrastructure, Utrecht) for his advice and support of this research, and to the following sponsors of the Building Materials research group at TU Eindhoven: Rijkswaterstaat Centre for Infrastructure, Graniet-Import Benelux, Kijlstra Betonmortel, Struyk Verwo, Attero, Enci, Provincie Overijssel, Rijkswaterstaat Directie Zeeland, A&G Maasvlakte, BTE, Alvon Bouwsystemen, V.d. Bosch Beton, Selor, Twee "R" Recycling, GMB, Schenk Concrete Consultancy, Geochem Research, Icopal, BN International, APP All Remove, Consensor, Eltomation, Knauf Gips, Hess AAC Systems, Kronos and Joma International (in chronological order of joining).

References

[1] L. Tang, Chloride transport in concrete – measurement and prediction. PhD Thesis, 1996, Chalmers University of Technology, Gothenburg, Sweden.
[2] C. Andrade, M.A. Sanjuan, A. Recuero, O. Rio, Calculation of chloride diffusivity in concrete from migration experiments, in non steady-state conditions, Cem. Concr. Res. 24 (1994) 1214–1228.
[3] L. Tang, Concentration dependence of diffusion and migration of chloride ions Part 1. Theoretical considerations, Cem. Concr. Res. 29 (1999) 1463–1468.
[4] L. Tang, Concentration dependence of diffusion and migration of chloride ions Part 2. Experimental evaluations, Cem. Concr. Res. 29 (1999) 1469–1474.
[5] A. Atkinson, A.K. Nickerson, The diffusion of ions through water-saturated cement, J. Mater. Sci. 19 (1984) 3068–3078.
[6] L.-O. Nilsson, M. Massat, L. Tang, Effect of non-linear chloride binding on the prediction of chloride penetration into concrete structures, ACI Special Publication, 145, 1994, pp. 469–486.

[7] J. Arsenault, J.P. Bigas, J.-P. Ollivier, Determination of chloride diffusion coefficient using two different steady-state methods: influence of concentration gradient, Proceedings of the International RILEM Workshop on Chloride Penetration into Concrete, 1995, pp. 150–160.
[8] T. Zhang, Chloride diffusivity in concrete and it measurement from steady state migration testing. PhD thesis, 1997, Trondheim University of Science and Technology, Norway.
[9] F. Nugue, S. Lorente, J.-P. Ollivier, Basis for the prediction of chloride ingress into cement-based materials, e-Mat — Revista de Ciência e Tecnologia de Materiais de Construção Civil 1 (1) (2004) 10–21.
[10] NT Build 492, Concrete, Mortar and Cement-based Repair Materials: Chloride Migration Coefficient from Non-steady-state Migration Experiments, Nordtest method, 1999.
[11] M.V.A. Florea, H.J.H. Brouwers, Chloride binding related to hydration products Part I: Ordinary Portland Cement, Cem. Concr. Res. 42 (2012) 282–290.
[12] H. Zibara, Binding of external chlorides by cement pastes. PhD Thesis, 2001, University of Toronto, Canada.
[13] E.M. Theissing, P.V. Hest-Wardenier, G. de Wind, The combining of sodium chloride and calcium chloride by a number of different hardened cement pastes, Cem. Concr. Res. 8 (1978) 683–692.
[14] P. Spiesz, M.M. Ballari, H.J.H. Brouwers, RCM: a new model accounting for the non-linear chloride binding isotherm and the non-equilibrium conditions between the free- and bound-chloride concentrations, Constr. Build. Mater. 27 (2012) 293–304.
[15] K.D. Stanish, The migration of chloride ions in concrete. PhD Thesis, 2002, University of Toronto, Canada.
[16] P. Spiesz, H.J.H. Brouwers, Influence of the applied voltage on the Rapid Chloride Migration (RCM) test, Cem. Concr. Res. 42 (2012) 1072–1082.
[17] Q. Yuan, Fundamental studies on test methods for the transport of chloride ions in cementitious materials. PhD Thesis, 2009, University of Ghent, Belgium.
[18] K. Krabbenhøft, J. Krabbenhøft, Application of the Poisson–Nernst–Planck equations to the migration test, Cem. Concr. Res. 38 (2008) 77–88.
[19] A. Delagrave, J. Marchand, E. Samson, Prediction of diffusion coefficients in cement-based materials on the basis of migration experiments, Cem. Concr. Res. 26 (12) (1996) 1831–1842.
[20] C. Andrade, Calculation of chloride diffusion coefficient in concrete from ionic migration measurements, Cem. Concr. Res. 23 (1993) 724–742.
[21] G.A. Narsilio, R. Li, P. Pivonka, D.W. Smith, Comparative study of methods used to estimate ionic diffusion coefficients using migration tests, Cem. Concr. Res. 37 (2007) 1152–1163.
[22] M. Castellote, C. Andrade, C. Alonso, Chloride-binding isotherms in concrete submitted to non-steady-state migration experiments, Cem. Concr. Res. 29 (1999) 1799–1806.
[23] C. Andrade, Concepts on the chloride diffusion coefficient, Proceedings of 3rd RILEM workshop on Testing and Modelling the Chloride Ingress into Concrete, Madrid, Spain, 2002, pp. 3–18.
[24] N. Otsuki, S. Nagataki, K. Makashita, Evaluation of the $AgNO_3$ solution spray method for measurement of chloride penetration into hardened cementitious matrix materials, Constr. Build. Mater. 7 (4) (1993) 195–201.
[25] R. Loser, B. Lotenbah, A. Leemann, M. Tuchschmid, Chloride resistance of concrete and its binding capacity — comparison between experimental results and thermodynamic modeling, Cem. Concr. Compos. 32 (2010) 34–42.
[26] NT Build 443, Concrete, Hardened: Accelerated Chloride Penetration, Nordtest method, 1995.
[27] K.D. Stanish, R.D. Hooton, M.D.A. Thomas, Prediction of Chloride Penetration in Concrete, US Department of Transportation, Federal Highway Administration, 2001. , (FHWA-RD-00-142).
[28] Z.F. Abu Hassan, Rapid assessment of the potential chloride resistance of structural concrete. PhD Thesis, 2012, University of Dundee, Scotland.
[29] C. Andrade, M. Castellote, C. Alonso, C. González, Relation between colourimetric chloride penetration depth and charge passed in migration tests of the type of standard ASTM C1202-91, Cem. Concr. Res. 29 (1999) 417–421.
[30] C.-C. Yang, C.T. Chiang, Relation between the chloride migration coefficients of concrete from the colourimetric method and the chloride profile method, J. Chin. Inst. Eng. 32 (2009) 801–809.
[31] M. Castellote, C. Andrade, C. Alonso, Accelerated simultaneous determination of the chloride depassivation threshold and of the non-stationary diffusion coefficient values, Corros. Sci. 44 (2002) 2409–2424.
[32] E. Gruyaert, Ph. Van den Heede, N. De Beile, Chloride ingress for concrete containing blast-furnace slag, related to microstructural parameters, Proceedings of the 2nd International RILEM Workshop on Concrete Durability and Service Life Planning Haifa, Israel, 2009, pp. 440–448.
[33] M. Maes, E. Gruyaert, N. De Belie, Resistance of concrete with blast-furnace slag against chlorides, investigated by comparing chloride profiles after migration and diffusion, Mater. Struct. 46 (2013) 89–103.
[34] D. Voinitchi, S. Julien, S. Lorente, The relation between electrokinetics and chloride transport through cement-based materials, Cem. Concr. Compos. 20 (2008) 157–166.
[35] A. Xu, S. Chandra, A discussion of the paper "Calculation of chloride diffusion coefficient in concrete from ionic migration measurements" by C. Andrade, Cem. Concr. Res. 24 (2) (1995) 375–379.